Thrust Control Algorithms for the GOCE Ion Propulsion Assembly

IEPC-2007-210

Presented at the 30th International Electric Propulsion Conference, Florence, Italy
September 17-20, 2007

M. H. Corbett*
QinetiQ Ltd, Cody Technology Park, Farnborough, GU14 0LX, U.K.

and

C. H. Edwards†
ESA-ESTEC, Keplerlaan 1, 2200 AG, Noordwijk ZH, The Netherlands

Abstract: The Gravity Field and steady-state Ocean Circulation Explorer (GOCE) mission seeks to characterize the short-term variation of the Earth's gravity field to high accuracy and high resolution, leading to improved gravity field and geoid models. GOCE will fly a near-circular, sun-synchronous, dawn-dusk orbit, with 96.5° inclination, at an altitude of around 250 km. The resulting atmospheric drag on the spacecraft leads to a number of thrust variation requirements for the ion propulsion assembly (IPA). The QinetiQ T5 ion thruster, as part of the Ion Propulsion Assembly (IPA) system, must be capable of providing thrust from 1 to 20 mN with a resolution of 12μN. In addition the system must conform to a series of drag modulation profiles expected as part of the mission life. This paper details the design optimization and test verification of the control algorithm used to meet these requirements. In particular, the paper describes how experimental data and theoretical understanding of the T5 ion thruster lead to a generic design that can be tailored to meet mission needs. Demonstrations of algorithm operation through simulation, and tests on flight representative hardware, are presented along with a brief discussion of the impacts of system component resolution on performance.

Nomenclature

A_r	=	Relative atomic mass of Xenon
B_P	=	Beam production cost
e	=	Electron charge
F_{am}	=	Actual measured thrust
F_d	=	Demanded thrust
F_{dm}	=	Filtered thrust demand for main flow control
$F_{dm\ n}$	=	Current value of Filtered thrust demand for main flow control
$F_{dm\ n-1}$	=	Previous iteration value of Filtered thrust demand for main flow control
F_{dIA}	=	Filtered thrust demand for anode current control
$F_{dIA\ n}$	=	Current value of Filtered thrust demand for anode current control
$F_{dIA\ n-1}$	=	Previous iteration value of Filtered thrust demand for anode current control
F_e	=	Electricaly determined thrust thrust

* Propulsion Scientist, Space Department, S&DU, EMEA, mhcorbett@qinetiq.com
† Electric Propulsion Engineer, TEC-MPE, clive.edwards@esa.int (formerly with QinetiQ)

F_{TF}	=	Thrust transfer function
$f_1(F_e)$	=	Thrust correction factor
$f_2(F_{dm})$	=	Magnet current gain schedule
$f_3(F_{dIA})$	=	Nominal anode current demand schedule
$f_4(F_{dm})$	=	Nominal main mass flow rate demand schedule
$f_5(F_{dm})$	=	Main mass flow rate correction to magnet current control schedule
$f_6(F_{dm})$	=	Anode current correction to magnet current control schedule
$f_7(F_{dm})$	=	Anode current filter constant schedule
I_A	=	Anode current
I_{Ad}	=	Anode current demand
I_B	=	Beam current
I_m	=	Magnet current
$I_{md\,n}$	=	Current iteration value of magnet current demand
$I_{md\,n-1}$	=	Previous iteration value of magnet current demand
k_i	=	Thrust transfer function coefficient
K_{Fdm}	=	Filter constant for main control
$\dot{m}_c$	=	Cathode mass flow rate
$\dot{m}_d$	=	Main mass flow rate demand
$\dot{m}_m$	=	Main mass flow rate
$\dot{m}_m(t)$	=	Main mass flow rate at time t
$\dot{m}_0$	=	Initial main mass flow rate
N_A	=	Avogadro's constant
t	=	Time
V_B	=	Beam voltage
ΔF	=	Thrust delta (i.e demanded thrust minus actual measured thrust)
ΔF_{corr}	=	Corrected thrust delta
ΔF_{dm}	=	Change in filtered thrust demand for main control from previous iteration
ΔI_{Ad}	=	Change in anode current demand
ΔI_m	=	Magnet current delta
ΔI_{Ad}	=	Change in anode current demand
ε	=	Main mass flow rate flow error
η	=	Propellant mass utilization efficiency
τ	=	Main mass flow rate step response time constant
τ_F	=	Filtered thrust for main control step response time constant

I.Introduction

The Gravity Field and steady-state Ocean Circulation (GOCE) mission plans to map the gravitational field of the earth to an accuracy of 1 to 2 mGal (10^{-5} ms^{-2}) with a spatial resolution of better than 100 km[1]. To measure this field, the spacecraft has, at its core, a 3-axis gradiometer, which will detect fluctuations in acceleration when operating at approximately 250 km above the Earth's surface. Operation at this altitude results in a retarding atmospheric drag on the forward velocity of the spacecraft, which must be compensated for, if adequate gradiometer measurement range and sensitivity is to be maintained.

To achieve adequate drag compensation, primary and redundant ion thruster systems are positioned at the opposite end of the spacecraft (as shown in Fig. 1). During measurement phases of the mission, the spacecraft control sends a series of thrust commands to the operating thruster

Figure 1. GOCE spacecraft

system, requiring the onboard ion thruster to react at a rate with high repeatability and minimum control hysteresis. The thruster chosen to meet these requirements is the QinetiQ T5.

This paper will detail the method used to determine the control algorithm design parameters for the flight thrusters, so that the drag profiles can be met. The theoretical basis for the algorithm design and the architecture of the algorithm are also described, incorporating experience and performance analysis techniques developed during the qualification model (QM) test program.

This paper presents some of the test results from the IPA level validation of the control algorithm operation. It will be seen that the algorithm behaved as expected, and that the process of translating thruster performance data into control parameters could be optimised in order to meet the challenging mission requirements.

II.GOCE Ion Propulsion Assembly (IPA)

A. Ion Propulsion Assembly Architecture

The IPA units are designed and assembled by EADS Astrium, with each assembly consisting of an EADS Astrium Crisa Ion Propulsion Control Unit (IPCU)[2], a Bradford Engineering Proportional Xenon Flow Assembly (PXFA), and a QinetiQ T5 Ion Thruster Assembly (ITA)[3].

Component units are positioned on a spacecraft floor as shown in Fig. 2. Both primary and redundant IPCUs are located on the face looking into the spacecraft, whereas the PXFA units are positioned above and below the ITA units on the face pointing out to space. The ITA units are mounted and aligned so that their nominal thrust vector is through the centre of mass of the spacecraft. Electrical and gas flow interfaces between each ITA and corresponding IPCU and PXFA are also on the external floor face.

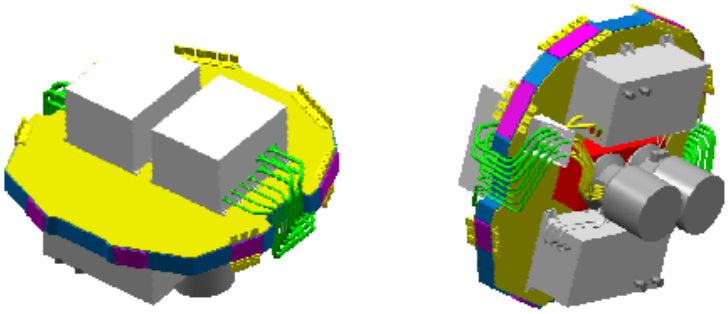

Figure 2. Ion Propulsion Assembly layout

B. T5 Ion Thruster Assembly (ITA)

The T5 ITA is a gridded Kaufman-type (ion bombardment) ion thruster, in which Xe gas is ionized in a cylindrical discharge chamber by means of an internal plasma discharge[4-6]. A schematic of the thruster is shown in Fig. 3. Plasma is created by the interaction of electrons flowing between the cathode and anode and the neutral mass flow. By applying an additional variable magnetic field a more efficient ionization process occurs, one that can be controlled to produce a range of discharge ionization conditions.

Output thrust is obtained by floating the discharge up to a high potential, typically above 1100 V, and extracting available ions through a set of grids. As the ion beam is neutralized on exit from the grids (by means of a neutralizing cathode), the accelerator grid is biased to a negative potential to prevent electrons back-streaming into the positively charged discharge plasma.

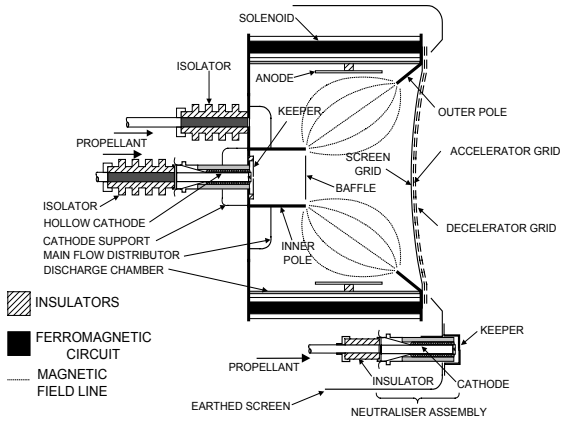

Figure 3. QinetiQ T5 ITA Schematic

III.Control algorithm overview

The purpose of the IPA control algorithm is to produce three parameter demands: main mass flow rate, anode current and magnet current, based on an input thrust demand. Each parameter demand is calculated using a sub-function as shown in the basic schematic in Fig. 4.

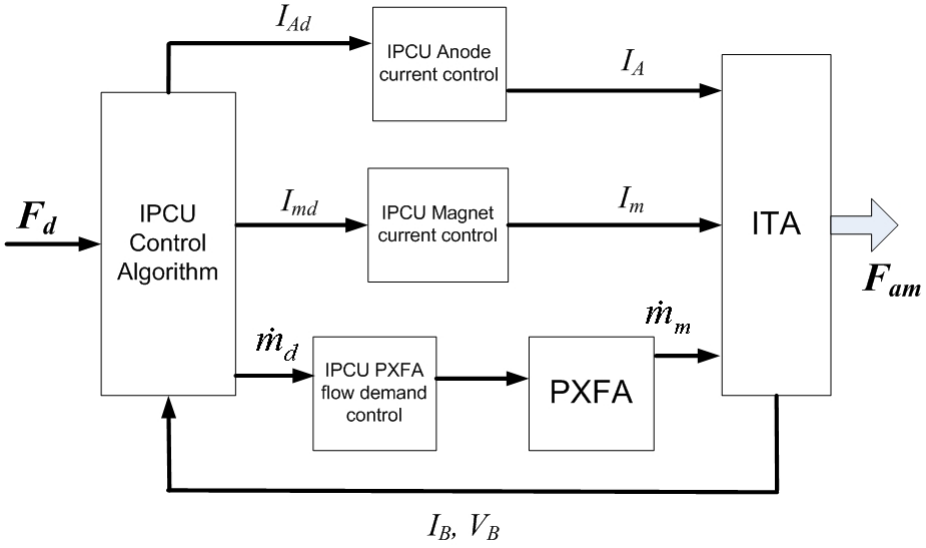

Anode and magnet current demands are relayed within the IPCU to power supplies, which then control the discharge current and magnetic field in the ITA. Main mass flow rate demand is sent to the PXFA, which responds by changing the flow input to the ITA. Main mass flow rate and anode current are controlled in open loop, whereas the magnet current is controlled in closed loop using feedback beam current and voltage telemetry. The sub-functions shown in Fig. 4 will be discussed in a later section.

IV.Achieving adequate Drag-free thrust

During measurement phases of the GOCE mission, the Drag-Free and Attitude-Control System (DFACS) will send a thrust demand to the IPA once every 100 ms (10 Hz). The maximum variation in this demand per 100 ms is 170 μN in the thrust range 1 to 3 mN, and 250μN in the thrust range 3 to 20 mN. For longer time scales the average variation rate decreases until the long-term thrust variation of 0.03 mNs^{-1}, for the thrust range 1 to 3 mN, and 0.07 mNs^{-1} for 3 to 20 mN.

The IPA has been designed to operate at a rate of 100 Hz, so that it can adequately achieve thrust control within each thrust demand period. The primary requirement is that the difference between the current and previous thrust demand i.e. demanded thrust step, is achieved to within ±12 μN of the step magnitude in 60 ms, and that this can be performed at any thrust level between 1 and 20 mN.

For the control algorithm to achieve this level of control, the IPCU and PXFA must have suitably accurate responses. Ideally the flow rate response would be fast and linear so that only a small variation of the electrical parameters need be performed. However the specified PXFA response is bounded by an envelope defined as a 1st order step with time constant τ between 0.4 and 10 s, having an offset, $\pm \varepsilon$, either 0.004 mgs^{-1} or 5% of the demanded flow rate:

$$\dot{m}_m(t) = \dot{m}_0 + (\dot{m}_d - \dot{m}_0)\cdot(1-\exp(-\frac{t}{\tau})) \pm \varepsilon \quad (1)$$

This relatively slow flow rate response means that achieving the required thrust range and precision control, over time scales of 1 to 30 s, is performed predominantly by varying the electrical parameters.

Given the above flow rate response, it is possible to achieve the required thrust control by varying the thruster's discharge electrical parameters. The functionality of the IPCU is therefore extremely important to achieving the required control resolution. In particular, this relates to the accuracy and resolution of the beam telemetry for closed

loop control, the software execution time between acquiring this telemetry and setting new power supply demands, and the accurate response of the power supplies. As a basic requirement, the IPCU processes should take under 10 ms to achieve, with as much time as possible between setting power supplies and reading the beam telemetry. In addition, the beam current telemetry should be accurate to at least 12-bit resolution and be characterised for long-term drifts.

Reduction in telemetry accuracy or slower electrical power supply response times will impact the ability to meet the required thrust response rate. Part of the control algorithm parameter optimization requires that aspects of the IPA system performance are considered, so that the full impact of the system is included. This will be discussed in a later section.

V. T5 ITA performance characterisation

C. Ground support equipment

For unit level characterization, the T5 is operated in a 3.8 m-diameter vacuum facility in pressures of less than 5 x 10^{-5} mbar, using purpose-built ground support equipment, similar to that used for the UK-10 ARTEMIS test program[7]. Two interconnected 19-inch racks, one containing low and high voltage power supplies, the other containing an array of HP/Agilent digital multimeters, are used to provide electrical input and to monitor data. The racks include shutoff interlocks and surveillance indicators to ensure user safety due to the high voltages employed when operating the thruster. Propellant flow is supplied using commercially available AERA flow controllers working in the 5 and 10 sccm (0 to 0.487 and 0 to 0.974 mgs^{-1}) range. All components are controlled at a rate of 1 Hz using customized software running on a standard personal computer.

In addition, a specially constructed independent Noise Electrical Ground Support Equipment (Noise EGSE) is incorporated into the set-up to measure the beam voltage and current to greater than 16-bit resolution at a rate of 1220 Hz. This device, consisting of a measurement unit connected to a PC running control software, is primarily operated in order to display real-time noise spectra within a bandwidth of 0.1 to 100 Hz. In general the fast acquisition rate provides high-resolution beam current data and, after suitable acquisition periods, is able to provide noise spectra for the required operation bandwidth of 1 mHz to 100 Hz.

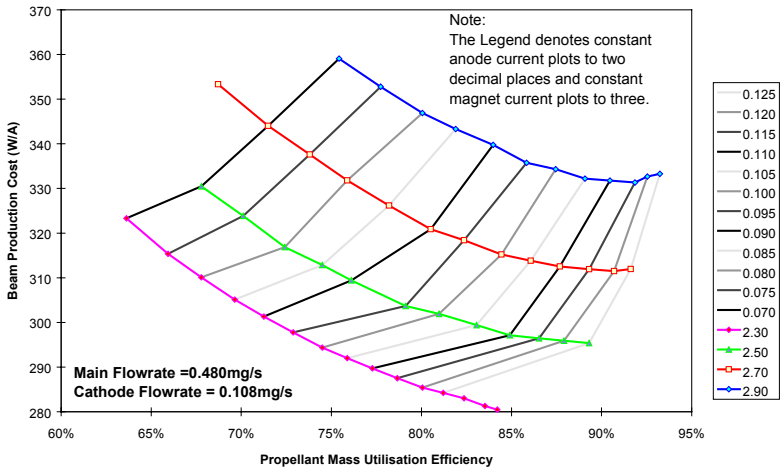

Figure 5. Propellant mass utilization efficiency against beam production cost for a T5 thruster at various anode and magnet current settings

The Noise EGSE was calibrated using thrust balance measurements performed during the qualification model (QM) phase of the GOCE ITA program. The Noise EGSE and the thrust balance were designed and built by The National Physics Laboratory, Teddington, UK.

D. Performance mapping

The T5 ITA performance envelope is characterised by adjusting the anode and magnet currents at various fixed mass flow rates until a predetermined limit criterion is reached. Examples of such limits are: beam current noise level; excessive anode voltage (which could lead to increased discharge chamber erosion); and accelerator grid impingement currents. Once these boundaries are set a more detailed performance characterization follows, leading to the creation of 'performance maps'. Such maps for the T5 have been described in literature before[6,8]. A common practice is to present the maps showing the mass propellant utilization efficiency, η, and beam production cost B_P

for various anode and magnet current settings (Fig. 5).

Electrical thrust values are calculated using Eq. (2), which represents the ideal thrust due to ion acceleration.

$$F_e = I_B \cdot \sqrt{\frac{2 V_B A_r}{N_A e}} \tag{2}$$

The beam current I_B is defined as:

$$I_B = \eta \, (\dot{m}_m + \dot{m}_c) \, \frac{N_A e}{A_r} \tag{3}$$

Actual measured thrust is then calculated by applying a thrust correction factor (f_1), which is determined from both theoretical analysis of thrust plume components and direct measurements on a thrust balance.

$$F_{am} = f_1(F_e) \cdot F_e \tag{4}$$

An output of performance characterization is the creation of nominal main mass flow rate and anode current 'schedules'. These are relationships, in the form of a look-up table, in which the parameter value is set depending on a required thrust level. In essence, it results in a thrust value being assigned to an individual performance map so that the maximum thrust variation can be achieved electrically. There are different methods, due to differing missions requirements, to how these values are assigned and how schedules are created. The GOCE requirements in particular represent a challenging set of specifications and the elected schedule determination method for the flight thrusters will be discussed in a later section.

VI.Detailed control algorithm design

E. Empirical thrust transfer function

The first step in the control algorithm design was the definition of an empirical thrust transfer function, F_{TF}, which was created from the performance characterization data. The form of the equation is quadratic relating magnet current to thrust (Equation 5), with coefficients being functions of mass flow rate and anode current.

$$\begin{aligned} F_{TF} &= k_1 \, (1 - \exp(k_2 \dot{m}_m)) \, I_m^2 + \\ &\left\{ k_3 \left(\dot{m}_m \cdot I_a\right)^2 + k_4 \left(\dot{m}_m \cdot I_a\right) + k_5 \left(\dot{m}_m \cdot I_a\right)^{\frac{1}{2}} + k_6 \right\} I_m + k_7 \, (1 - \exp(k_8 \dot{m}_m)) \end{aligned} \tag{5}$$

$$\frac{\partial F_{TF}}{\partial I_m} = 2 k_1 \left(1 - \exp(k_2 \dot{m}_m)\right) I_m + \left[k_3 (\dot{m}_m \cdot I_a)^2 + k_4 \left(\dot{m}_m \cdot I_A\right)^{\frac{1}{2}} + k_5 \left(\dot{m}_m \cdot I_A\right) + k_6 \right] \tag{6}$$

$$\frac{\partial F_{TF}}{\partial I_A} = \left[2 k_3 \dot{m}_m{}^2 I_A + \frac{k_4}{2} \sqrt{\left(\frac{\dot{m}_m}{I_A} \right)} + k_5 \dot{m}_m \right] I_m \tag{7}$$

$$\frac{\partial F_{TF}}{\partial \dot{m}_m} = \left[2 k_3 \dot{m}_m \, I_A^2 + \frac{k_4}{2} \sqrt{\left(\frac{I_A}{\dot{m}_m} \right)} + k_5 I_A \right] I_m - I_m{}^2 \, k_1 \, k_2 \exp(k_2 \dot{m}_m) - k_7 \, k_8 \exp(k_7 \dot{m}_m) \tag{8}$$

The partial derivatives of the transfer function, F_{TF}, illuminate the underlying thrust dependence on individual

control parameters. Table 1 provides a series of nominal operation setting ranges from the QM ITA performance characterization data, and using Eqs. (6) to (8), the effect of varying each input parameter on output thrust can be reasonably approximated.

These empirical transfer functions were used to create a thrust response control strategy based on empirical data, rather than using a detailed plasma model derived from first principles.

Table 1. QM ITA performance envelope and thrust transfer function coefficients

$\dot{m}_m$ (mgs^{-1})	I_A (A)	I_m range (A)	*Thrust transfer function coefficients (units not included)*
0.033	0.124	0.075 to 0.150	k_1 = -240
0.044	0.173	0.075 to 0.151	k_2 = -7.2
0.063	0.360	0.075 to 0.155	k_3 = 8
0.100	0.723	0.075 to 0.163	k_4=145
0.135	0.978	0.072 to 0.174	k_5=-42
0.202	1.400	0.055 to 0.194	k_6= 8
0.282	1.750	0.050 to 0.250	k_7= 0.418
0.327	2.043	0.050 to 0.250	k_8= -14.3
0.395	2.490	0.050 to 0.250	
0.462	2.969	0.050 to 0.250	
0.480	3.000	0.050 to 0.250	

The typical operational procedure during characterization is to vary the mass flow rate first, followed by the anode current, and finally the magnet current. This is due largely to dynamic effects in the ground support equipment. It takes longer for the discharge voltage to settle after large anode current variations than occurs when varying the magnet current in the same proportion, and large flow rate changes (> 0.2 mgs^{-1}) are only achieved on time scales of the order of 5 to 10 s.

For faster response times to thrust variations, smaller increments in the anode current or flow rate are necessary with the magnet current becoming the dominant control parameter. In terms of a control hierarchy therefore, the parameters would be ranked magnet current, anode current and mass flow rate in order of impact on thrust variation.

Analysis of the output data from Eqs. (6) to (8), reveals that the anode current makes a significant contribution to thrust variation at low mass flow rates, which reduces on increasing flow rate. For the mass flow rate range shown in Table 2, there is an increasing thrust contribution due to anode current below approximately 0.3 mgs^{-1}. The magnet current continues to have an impact but the implication is that anode current variation will need to be included if the required thrust response is to be achieved. This is not surprising as other thruster test measurements show that the thrust range due to electrical parameter variation decreases for lower flow rates and thrust variation due to magnet current variation becomes comparable to that achieved by varying the anode current.

There is also a thrust variation due to changing the flow rate, which needs to be included in the control strategy. However this is expected to be smaller in magnitude than any anode current induced variation, as the flow rate increment per iteration is very small due to the slow flow rate response (Eq. (1)).

F. Open loop and closed loop algorithms

As described in section III, the control algorithm was designed to have two functions, open loop control and closed loop throttling. In addition, simple relationships were to be used where possible to allow for parameter optimization during testing. The core of the algorithm is the association of nominal thrust with main mass flow rate, where nominal thrust is created by filtering the thrust demand. This is achieved using a linear difference equation that approximates a 1st order step function with a time constant of 10s, over time intervals of t = 10 ms. The value of K_{Fdm} is 0.001.

$$F_{dm\,n} = F_{dm\,n-1} + (F_d - F_{dm\,n-1}) \cdot (1 - \exp(-\frac{t}{\tau_F})) \approx$$

$$F_{dm\,n-1} + (F_d - F_{dm\,n-1}) \cdot \frac{t}{\tau_F} = F_{dm\,n-1} + K_{Fdm}(F_d - F_{dm\,n-1}) \quad (9)$$

A similar filter is applied to anode current demand,

$$F_{dIA\ n} = F_{dIA\ n-1} + f_7(F_{dm})\left(F_d - F_{dIA\,n-1}\right) \tag{10}$$

The schedule f_7 is designed so that the filter response is variable over the thrust range, as (which will be shown later) the anode current needs to be throttled in larger steps at low thrust levels than at higher thrust levels. As this variation in response is related to main mass flow rate, f_7 is dependent on F_{dm}. At higher flow rates the filter function tends to the value of 0.001 reflecting the gradual simplification of the algorithm into proportional magnet current control.

These two filters are used to set the open loop anode current demand and mass flow rate demand by using their nominal schedules, respectively f_3 (F_{dIA}) and f_4 (F_{dm}). This information is then passed into the closed loop control calculations.

Due to the dominance of magnet current on thrust variation, the simplest form of closed loop control is proportional control between magnet current variation and measured thrust delta

$$\Delta I_{md} = f_2(F_{dm})\Delta F = f_2(F_{dm})\left(F_d - F_{meas}\right) \tag{11}$$

The schedule f_2 reduces for increasing mass flow rate, hence increasing nominal thrust F_{dm}, reflecting the fact that the available thrust range increases for the same magnet current increment.

At this point, one can see how there would be three simultaneous parameter demands that proceed independently of each other. In order to meet the thrust response requirement, provision must be made for the effect on thrust of varying the anode current and the main mass flow rate before throttling the magnet current. If this is not done the combined thrust response will overshoot the step demand in certain thrust ranges, particularly at low thrust levels.

Instead of controlling to ΔF, the contribution from the other parameters is included so that the magnet current uses a corrected thrust delta, ΔF_{corr}

$$\Delta I_{md} = f_2(F_{dm})\Delta F_{corr} = f_2(F_{dm})\left(\Delta F - f_5(F_{dm})\Delta F_{dm} - f_6(F_{dm})\Delta I_{Ad}\right) \tag{12}$$

The magnet current demand is then the previous demand plus the newly calculated magnet current delta.

$$I_{md\,n} = I_{md\,n-1} + \Delta I_{md} \tag{13}$$

The selection of ΔF_{dm} for thrust correction due to flow rate in Eq. (12), rather than a change in main mass flow rate demand, was an arbitrary choice during the development of the algorithm. The schedule f_5 could be as easily defined with main mass flow rate as the independent variable. The change in anode current demand, ΔI_{Ad}, is the anode current demand, generated from the f_3 function, minus the previous iteration demand.

Equations (9) to (13) represent the basic GOCE ITA thrust control algorithm and are shown in context in Fig. 6. Additional anode and magnet current minimum and maximum limit schedules were added in the initial design and are still included in the flight algorithm though they are

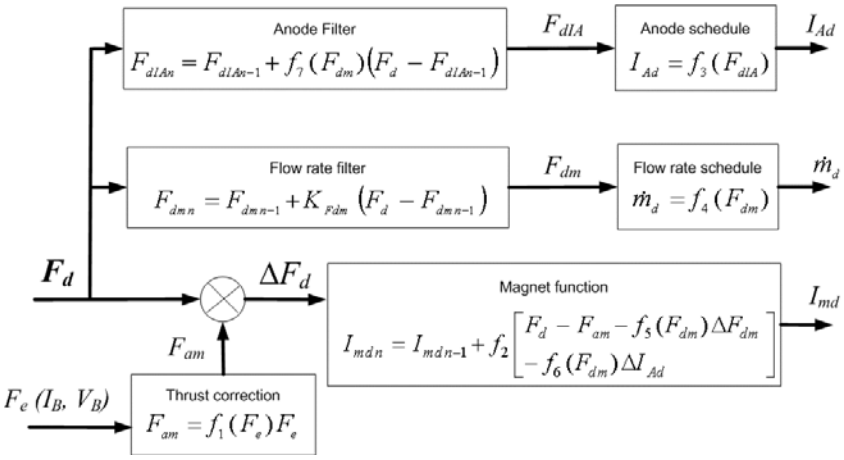

Figure 6. Control algorithm schematic with equations

not necessary to ensure stable thruster operation.

G. Nominal anode current and main mass flow rate schedule determination

The detailed performance characterization for the flight thrusters was carried out using a strategy defined by the thrust variation requirements and the control algorithm design. The operational envelope limits were defined initially for various main mass flow rates up to approximately 0.56 mgs^{-1}. At each fixed value of main mass flow rate, the anode current range was divided into 5 equally spaced values, and the magnet current range defined for each value. To determine the flight f_3 and f_4 schedules, the open loop control functionality of the algorithm was calculated using an initial f_3, f_4 and f_7 estimate based on QM testing, and worst-case thrust ramp profiles. These profiles are the fastest ramp to 20 mN from 1 mN and from 20 mN to 1 mN following the thrust variation requirements.

Inputting thrust demand and filtering it generated the main mass flow rate and anode current demands. The actual mass flow rate being supplied to the thruster was calculated using Eq.1. With these two values, a magnet current range was obtained by linearly interpolating between the operational envelope data points. By adjusting values in f3 and f4 and by introducing the worst-case errors in mass flow rate, a pair of schedules can be determined that give the maximum thrust variation capability. Errors and lag in main and cathode flow rates between demanded and actual flow rate are by far the biggest factors that effect thrust variation capability.

In parallel to this schedule determination activity, 'performance mapping' of the thruster was carried out. The resulting data set then replaced the initial operational envelope data and the schedules were checked against thrust performance. The final f3 and f4 schedules were then obtained.

Figure 7 shows a series of simplified performance maps for the GOCE T5 ITA Flight Models, plotting beam current against magnet current at main mass flow rates of 0.091, 0.238 and 0.511 mgs^{-1}. In all cases, cathode flow rate is fixed at 0.11 mgs^{-1}. As in Fig. 5, each curve in the plot represents a different anode current setting within operational boundaries.

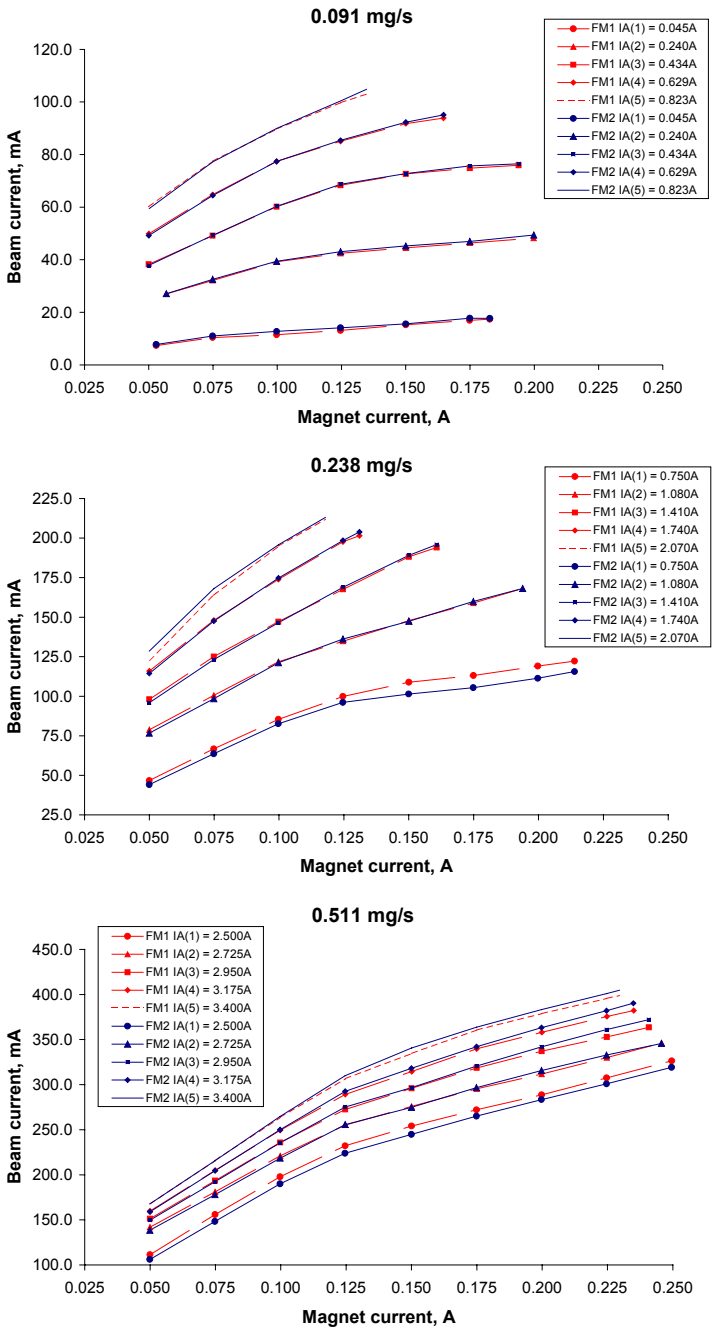

Figure 7. Performance maps showing measured beam current versus input magnet current at various anode currents (legend) and main mass flow rate settings (titles)

VII. Simulation model

In order to optimize the control algorithm closed loop-throttling behavior a MatLab/Simulink™ model was used that represents key functionalities of the IPA units. This is shown schematically in Fig. 8. The IPCU model includes software execution timing, dynamic responses of the anode, magnet and beam supplies and the control algorithm architecture. The PXFA model is a 1st order step function according to Eq. (1).

To minimise the model inaccuracy, the ITA simulation uses a set of polynomial trends derived from the performance data, rather than a single transfer function. To produce this set, the performance data is divided into 35 sub-sets, each of which is labelled by a magnet current value (0.050 to 0.250 A in 0.025A steps) and an anode current rank. When each performance map was measured the anode current range was divided equally into 5 parts, ranked lowest to highest, so rank 1 refers to the set of all performance data at the lowest anode current values, and so forth. The magnet current values stay the same over the performance envelope, where as the anode current values change in magnitude but not in rank. Therefore, provided there is a reference table matching anode current value with rank, it is possible to select a sub-set of data for a given value of main mass flow rate.

For example, Fig 9 depicts two performance maps at two different mass flow rates 1 and 2. Polynomial 1 represents the relationship between thrust and mass flow rate for a magnet current value of 0.150A and all rank 1 anode current values, polynomial 2 is the trend at I_m = 0.075A, I_A = rank 2 values, polynomial 3 is the trend at I_m = 0.150A, I_A = rank 3 values and polynomial 4 is the trend at I_m = 0.125A, I_A = rank 5 values. The anode current values would be read from the reference table such that rank 1 is the first column of anode current data, rank 2 the next column, and so forth. At all times it is possible to relate input magnet current and anode current to a region of the envelope falling between, at most, four trends. In practice, at lower mass flow rates, there may not be thrust values at some of the highest magnet current values. When creating the polynomial trends, data is simulated at these values according to the observed thrust behaviour so that the polynomials will all use the same number of points for fitting. Data boundaries are then applied so that these simulated regions do not get selected in the ITA model.

The output thrust is calculated by linearly interpolating between the polynomials. The first stage of the process is to select 4 polynomials to bound the input magnet current and anode current. Four thrust values are calculated by inputting mass flow rate, and these values are then reduced to a single thrust value by linearly interpolating using scale factors derived from the input parameters.

The polynomial map does not have equal granularity for all values of mass flow rate, since anode current relationships are used rather than absolute values of anode current. However, the thrust variation due to anode and magnet current variation becomes more linear as flow rate increases (Fig. 7), so this balances what appears to be decreasing data resolution. The derivation and referencing method reflects the performance mapping technique and was found to be sufficient in predicting thruster behaviour as long as the acquisition of measurement data was performed with the same ground

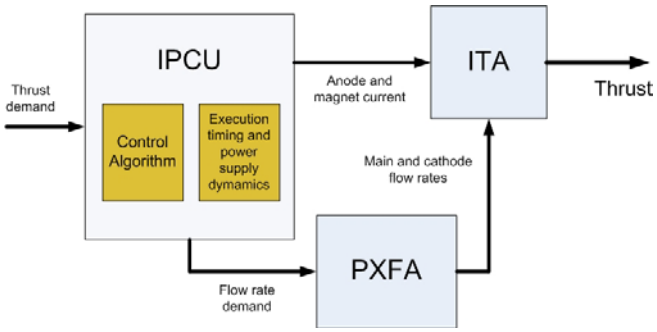

Figure 8. Schematic of Control Algorithm simulation used to optimize schedules

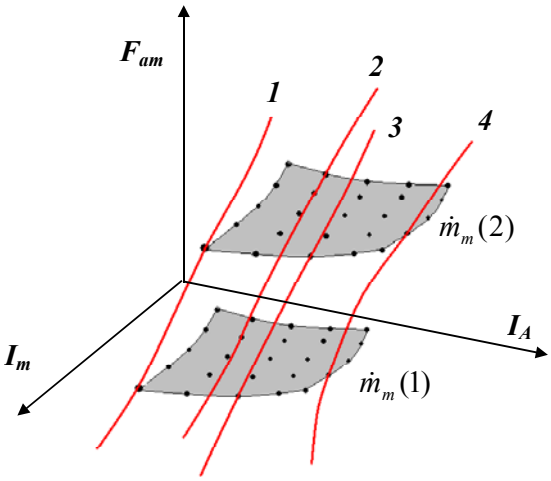

Figure 9. A schematic of polynomial trend fitting to ITA performance data. Each polynomial (1 to 4) represents a relationship between thrust and mass flow rate according to a particular set of anode current values and a fixed value of magnet current.

support equipment and in the same manner for all performance maps. For the FM1 data the worst-case model inaccuracy was 5.7% for an outlying data point. The average inaccuracy of the model was less than 1%.

H. Simulation results

The FM2 ITA performance data was found to be almost identical to that for FM1 (as shown in Fig. 7), accounting for thermal effects due to the time line of the performance mapping process. Hence, only FM1 ITA control algorithm parameter optimization was performed, as with reasonable confidence, the schedules obtained for FM1 would be applied to FM2.

To optimize the throttling schedules, f_2, f_5 and f_6, a series of ramps were performed starting at various thrust levels from 1 to 20 mN. Each ramp was designed to test thrust variation over a specific time base. Tests varied from a series of single steps to 60 s variations of 0.07 mNs^{-1}. Figure 10 shows a few examples of ramps and how the simulated thrust varies with demand. Control algorithm schedules were deemed optimized when all tests passed the thrust response criteria of total thrust variation over its corresponding time interval.

I. Model sensitivity and accuracy

The basic IPA simulation used to define schedules does not fully represent the flight IPA, in that some flight parameter resolutions and accuracies are not included. The reason for this is that some of the parameter resolutions directly impact the ability of the algorithm to meet thrust requirements and do so regardless of the values of the schedule parameters. When defining schedules, a simulation with accuracies and resolutions representing the ground support equipment is used to minimise the impacts of incorrect schedules on thruster performance, with the only exception being the variation in flow rate defined in Eq. (1).

For the QM ITA program a further sensitivity analysis was performed that included various specified flight power supply setting accuracies, resolutions and feedback telemetry. The main parameters that directly affect thrust variation were found to be accuracy of the beam current telemetry and to a lesser extent the accuracy of the beam voltage telemetry. This should not come as a surprise, however, as the closed loop control depends on the beam current and voltage telemetry to calculate the actual thrust delta between demand and output thrust.

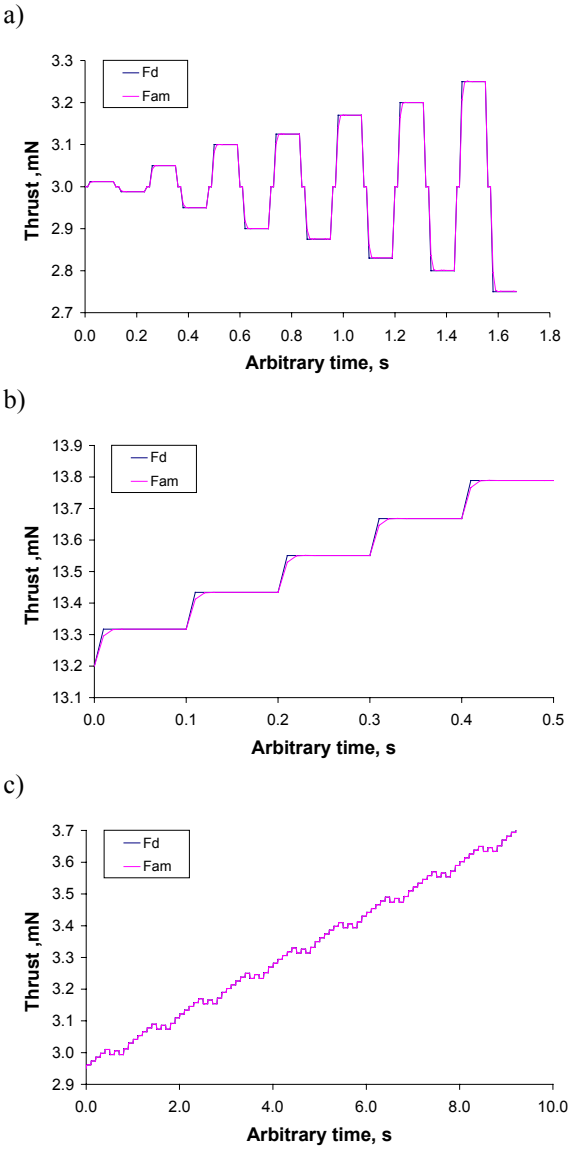

Figure 10. Demanded thrust F_d and simulated actual measured thrust F_{am} for thrust ramps a) A series of single steps from 3.0 mN b) a train of 5 steps of 117 µN c) 0.080 mN/s ramp rate using combinations of 12 µN steps from 2.95 mN. All variations are with a PXFA time constant of 10 s

An estimate of thrust inaccuracy can be made directly from Eq. (2): An expected error of 1 mA of beam current corresponds to approximately 55 µN of constant thrust error, where as an expected inaccuracy on 1.5V in the 1176V beam voltage produces a relationship of 1.25 µN error per mN of output thrust. At 20 mN, this error is 25 µN. From these relationships, thrust response inaccuracy can be directly related to beam current telemetry inaccuracy alone with reasonable certainty.

VIII. Flight system results

The GOCE IPA was tested in QinetiQ between December 2006 and June 2007. The tests were performed to verify functional and performance requirements for the various component units and to characterise the IPA behaviours. Among the requirements associated with the ITA was control algorithm performance.

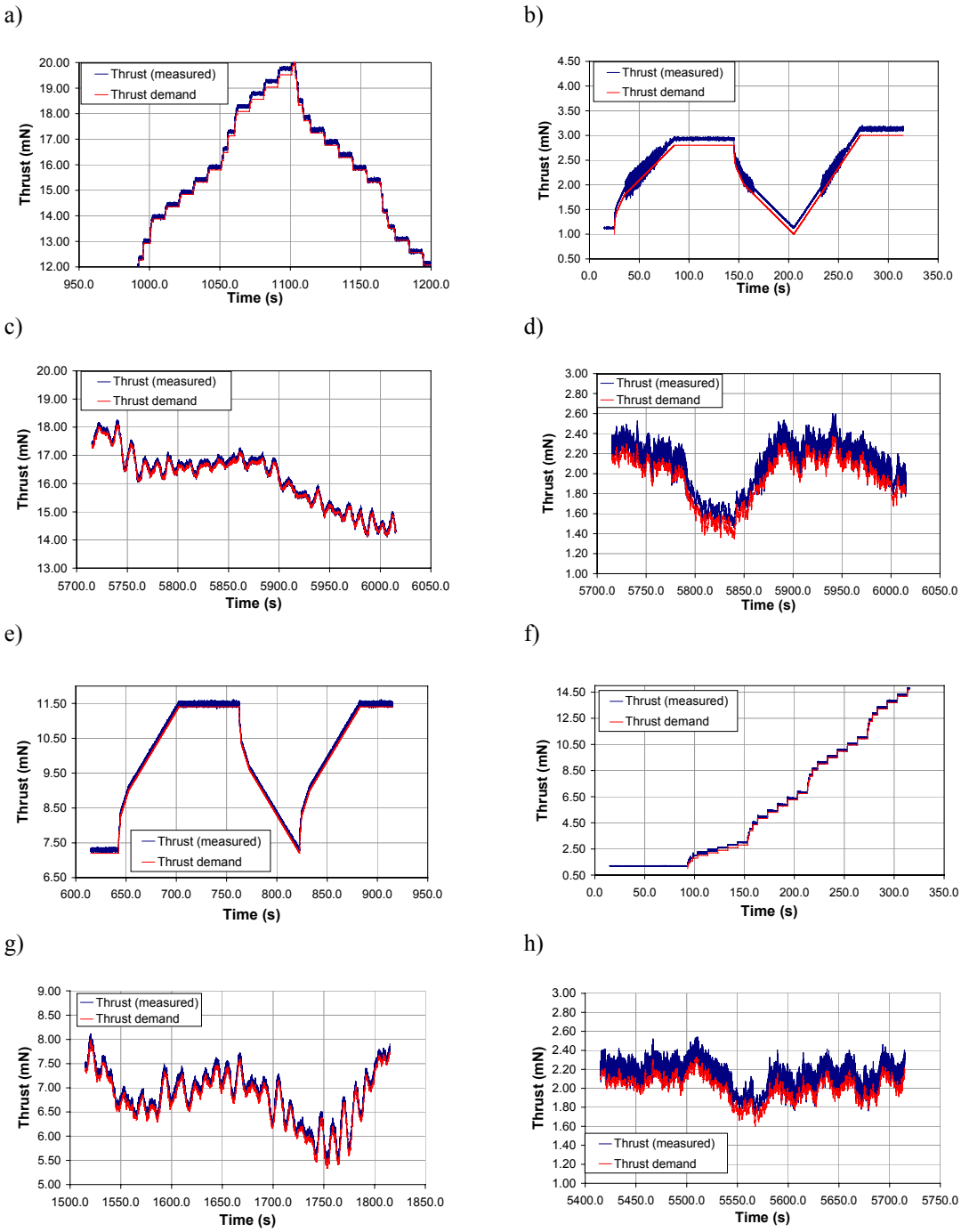

Figure 11. Sections of various flight system thrust profiles showing demanded thrust and actual measured thrust, derived from data acquired on the NPL Noise EGSE, for IPA 1 a) to d) and IPA 2 e) to h). Note that the time shown is relative to the start of full individual profiles.

Figure 11 shows various graphs depicting demanded thrust and measured thrust obtained using the Noise EGSE (after correction for equipment calibration and the thrust correction factor f_1). In all graphs, a clear positive thrust offset can be seen that occurs due to a negative telemetry offset. In this situation the algorithm is continually increasing the magnet current demand above the level required to meet the thrust demand as the feedback beam current telemetry is telling the algorithm that the output thrust is still too low. From a spacecraft point of view this offset is corrected by simply demanding slightly less thrust.

For thrust ramps in the 1 to 3 mN thrust range (Fig. 11b) there are regions with slightly higher thrust noise than other thrust levels in the profile. Though this noise does not exceed requirements, it does mask the lower frequency control behaviour, unless multiple ramps are performed and the data averaged.

The thrust profiles shown in Fig. 11 represent some of the possible drag profiles that the IPA will receive from DFACS, and some profiles that are allowable permutations of the drag free requirements. These profiles can be a series of coarse thrust steps (Fig. 11a and 11f), a series of ramps (Fig 11b and 11e) or a series of fine thrust variations (Fig 11c, 11d, 11g and 11h). In general, the control algorithm was observed to function correctly within the achievable measurement resolution and within the general ITA performance envelope characteristics. This is including thrust noise and correcting for the observable thrust offset. No deviations from thrust profiles or saturation effects outside of requirements were observed.

Hence the preliminary conclusion is that the process of defining flight schedules using unit level testing and simulation, with respect to specific thrust variation requirements, is sufficient to produce correct flight operation without need for subsequent parameter adjustment.

IX. Conclusion

This paper shows, to a reasonable degree of certainty, that it is possible to test a T5 ion thruster (or by association, a T6) with in-house test equipment and use this data to successfully operate and control that thruster to very high resolution on a flight system. In order to achieve this, a generic control algorithm was designed that incorporated the effect of variation of mass flow rate, anode current and magnet current on output thrust. Rather than design a plasma model from first principles, thruster performance data was collected using a specific measurement strategy, which allowed an accurate thruster simulation to be created. The output of the simulation analysis was a set of control schedules that could be used to control the thruster in flight configuration.

References

[1]Haagmans R., Floberhagen R., Pieper B., Drinkwater M., Rider H., Rast M and Battrick B., "GOCE ESA's Gravity Mission", ESA BR-209, ESA Publications Division, Noordwjik, The Netherlands, June 2006

[2]Tato, C., Palencia, J. and de la Cruz, F., "The Power Control Unit for the Propulsion Engine of GOCE Program", *Proceedings of the 4th International Spacecraft Propulsion Conference,* ESA SP-255, Editor: A. Wilson, Published on CD-ROM, 2004.

[3]Edwards, C. H., Wallace, N. C., Tato, C and van Put, P., "The T5 Ion Propulsion Assembly for Drag Compensation on GOCE", *Second International GOCE User Workshop "GOCE, The Geoid and Oceanography ESA-ESRIN,* ESA SP-569, ESA Publications Division, Noordwjik, The Netherlands, June 2004.

[4]Fearn, D. G., Martin, A. R. and Smith, P, "Ion Propulsion Research and Development in the UK", *Journal of the British Interplanetary Society*, Vol. 43, 1990, pp 431-442.

[5]Fearn, D. G., "The UK-10 Ion Propulsion System – a Technology for Improving the Cost-Effectiveness of Communications Spacecraft", *AIDAA / AIAA / DGLR / JSASS 22nd International Electric Propulsion Conference*, IEPC-91-009, 1991.

[6] Fearn, D. G., Martin, A. R. and Smith, P, "Ion Propulsion Development in the UK", *AIAA / SAE / ASME / ASEE 29th Joint Propulsion Conference and Exhibit*, AIAA 93-2063, AIAA, Washington, D.C, 1993.

[7]Mundy, D. and Fearn, D. G., "Throttling the T5 Ion Engine over a Wide Throttling Range", *AIAA / SAE / ASME / ASEE 33rd Joint Propulsion Conference and Exhibit*, AIAA-1997-3196, AIAA, Washington, D. C., 1997.

[8]Edwards, C. H., "Life Testing of the UK-10 Ion Propulsion System at MMS Portsmouth", *2nd European Spacecraft Propulsion Conference,* ESA SP-398, ESA Publications Division, Noordwjik, The Netherlands, August 1997, pp 701-706